Combined HREELS and Raman study of GaAs-AlAs superlattices

T. Tsuruoka, M. Sekoguchi,* Y. Uehara, and S. Ushioda
Research Institute of Electrical Communication, Tohoku University, Sendai 980, Japan

T. Kojima and K. Ohta
Electrotechnical Laboratory, 1-1-4, Umezono, Tsukuba, Ibaraki 305, Japan
(Received 2 November 1993)

GaAs-AlAs superlattices have been investigated by combining high-resolution electron-energy-loss spectroscopy (HREELS) and Raman spectroscopy. The superlattices were grown on GaAs(100) substrates by molecular-beam epitaxy. The sample surface was protected by an As capping layer formed *in situ* after growth, so that a well-ordered surface could be obtained by heating the sample mildly in UHV prior to HREELS measurements. The experimental results were compared with the dielectric theory of HREELS reported by Lambin *et al.* [Phys. Rev. B **32**, 8203 (1985)]. The TO phonon frequencies and damping constants of GaAs and AlAs of individual samples, required for the theoretical calculations, were determined by Raman-scattering measurements. Excellent agreement was obtained between the theoretical and experimental results for all the samples with different layer thicknesses and for all the electron impact energies (from 4 to 35 eV) observed.

I. INTRODUCTION

Recently there has been considerable interest in the properties of well-controlled layered structures of III-V and II-VI semiconductors that can be grown by molecular-beam epitaxy (MBE) and metal-organic chemical-vapor deposition. To understand the properties of such structures, it is useful to investigate the elementary excitations that are localized at the top surface and the interfaces in the structure. This is because the properties of the elementary excitations are very sensitive to the layer thickness, the sharpness of the interfaces, and the dielectric response of the materials that make up the layers.

High-resolution electron-energy-loss spectroscopy (HREELS) is a powerful technique for investigating the vibrational and electronic properties of such structures. In this technique, the probing depth into the sample surface can be varied by changing the electron incidence angle and the impact energy. Thus, by HREELS one can probe the elementary excitations localized at interfaces below the surface of multilayered structures.

To obtain useful information from the high-resolution electron-energy-loss (HREEL) spectra, one needs a detailed theory of the spectra to compare with experimental results. In the case of adsorbed molecules[1] and oxide layers,[2] the HREEL spectra for the specular configuration could be reproduced with good accuracy by a macroscopic dielectric theory. For superlattices and general layered structures, the dielectric theory of HREELS was developed by Lambin, Vigneron, and Lucas.[3] Thiry *et al.* applied HREELS to GaAs-$Al_{0.3}Ga_{0.7}As$ superlattices[4] and InAs-GaSb superlattices.[5] They attempted to compare their experimental results with the dielectric theory reported by Lambin, Vigneron, and Lucas. However, a rigorous comparison between the theory and experiment was difficult, because of the ambiguities on the thickness and the stoichiometry of the topmost layer. The ambiguities were caused by the use of argon-ion bombardment in cleaning and thinning the top layer of the samples.

Gray-Grychowski *et al.* adopted an As overlayer technique to protect the GaAs surface from contamination in air.[6] They deposited amorphous As on the sample surface while the sample was still in a MBE chamber. Using this technique, they could transfer the sample from the MBE chamber to a HREELS chamber through atmosphere without any contamination of the sample surface. The As capping layer was removed by heating the sample in the HREELS chamber. By this technique, a damage-free and clean GaAs surface could be prepared.

In the present work, we have investigated the surface and interface phonon polaritons in GaAs-AlAs superlattices by HREELS. We fabricated As capped GaAs-AlAs superlattices by MBE. Thus, a clean surface was obtained by heating the sample mildly in the HREELS chamber even though it was exposed to air. Then, HREEL spectra were measured and compared with the dielectric theory. The TO phonon frequencies and the damping constants of the GaAs and AlAs layers required for the theoretical calculations were determined by Raman scattering for individual samples.

The present paper consists of six sections. In Sec. II a brief summary of the dielectric theory is presented, and the experimental details are described in Sec. III. The experimental results are presented in Sec. IV, and the experimental and theoretical results are compared in Sec. V. Section VI is the conclusion.

II. THEORY

In this section we present a brief summary of the dielectric theory of HREELS. The description is restricted to the parts required for the numerical calculations of

HREEL spectra for our superlattices. The scattering geometry and the superlattice structure are illustrated in Fig. 1. E_0 is the incident electron energy; θ is the incident angle measured from the surface normal; Φ_a is the half acceptance angle of the analyzer. The GaAs and AlAs layers are deposited alternately on a GaAs(100) substrate, with different dielectric function $\varepsilon_A(\omega)$ and $\varepsilon_B(\omega)$, and layer thicknesses d_A and d_B, respectively. The space above the structure is filled with vacuum. The topmost layer is GaAs. L is the thickness of one period ($L=d_A+d_B$) and p is the total number of the periods.

We will follow the theory by Lucas and Sunjic who derived the quantum-mechanical multiple-energy-loss probability $P_i(\omega)$ at temperature T.[7] It is given by

$$P_i(\omega)=\frac{1}{2\pi}\int_{-\infty}^{\infty} dt\,\exp(i\omega t)\times\exp\left[-\int_0^{\infty} P_{\rm cl}(\omega')\coth\left[\frac{\hbar\omega'}{2k_BT}\right]\times(1-\cos\omega' t)\,d\omega' - i\int_0^{\infty} P_{\rm cl}(\omega')\sin\omega' t\,d\omega'\right], \quad (1)$$

where k_B is the Boltzmann constant and $P_{\rm cl}(\omega)$ is the classical energy loss probability that describes a single scattering.

Let us consider an electron that travels with velocity $\mathbf{v}_e(t)$ on a fixed trajectory $\mathbf{r}_e(t)$ illustrated in Fig. 1. The incident electron interacts with a long-ranged electric field induced by the fluctuation of the electric dipole moment on the surface. The dipole scattering is dominant in the specular scattering geometry. In this case, the HREEL spectrum can be treated within the macroscopic dielectric theory.[8] The work W done by the induced electric field $\mathbf{E}_p(\mathbf{r},t)$ on the electron is

$$W=\int_{-\infty}^{+\infty} e\mathbf{E}_p([\mathbf{r}_e(t),t])\cdot\mathbf{v}_e(t)dt\ . \quad (2)$$

In terms of $P_{\rm cl}(\omega)$, W can be written

$$W=\int_0^{\infty} P_{\rm cl}(\omega)\hbar\omega\,d\omega\ . \quad (3)$$

Thus, $P_{\rm cl}(\omega)d\omega$ represents the probability that the electron loses energy $\hbar\omega$ by emission of one quantum of a surface excitation at zero temperature in the scattering process.

According to Lambin, and co-workers[3,9] $P_{\rm cl}(\omega)$ is given by

$$P_{\rm cl}(\omega)=\frac{4}{\pi^2}\frac{e^2}{4\pi\varepsilon_0\hbar}\int\int\frac{[kv_\perp f(kL_i/2)]^2}{[(kv_\perp)^2+(\mathbf{k}\cdot\mathbf{v}_\parallel-\omega)^2]^2}\times{\rm Im}\left[\frac{-1}{\xi(\mathbf{k},\omega)+1}\right]\frac{d^2k}{k}\ , \quad (4)$$

where $v_\parallel$ and $v_\perp$ are the components of the electron velocity parallel and perpendicular to the surface, respectively; $\mathbf{k}$ is the surface parallel component of the wave vector of the surface excitation. The factor $[f(kL/2)]^2$ accounts for the reduction of the interaction time due to the additional attraction by the image potential.[9] It causes the lowering of inelastic intensities for grazing incidence. f is a universal function given by

$$f(u)=u\,[K_i(u)-K_0(u)]e^u\ , \quad (5)$$

where K's are the modified Bessel functions of the second kind. L_i is a characteristic length determined by the image potential; it is given by

$$L_i=\alpha e^2/2mv_\perp^2\ , \quad (6)$$

where α is the screening factor appropriate to a material under investigation. We see the integrand in Eq. (4) is composed of a product of two terms. The first term that depends on the geometrical configuration of the measurement and the speed of the electron is called the kinematic prefactor. It takes the maximum when the surfing condition $\mathbf{k}\cdot\mathbf{v}_\parallel=\omega$ is satisfied. The remaining term is called the surface loss function. It represents the dielectric response of the sample to the incident electron.

$\xi(\mathbf{k},\omega)$ is the effective dielectric function of the sample system. When the sample is a single crystal, it corresponds to the dielectric function $\varepsilon(\omega)$ of the crystal. For a superlattice with the periodic structure of Fig. 1, the effective dielectric function $\xi(\mathbf{k},\omega)$ is expressed by a continued fraction

$$\xi(k,\omega)=a_1-\cfrac{b_1^2}{a_1+a_2-\cfrac{b_2^2}{a_2+a_3-\cfrac{b_3^2}{a_3+a_4-\cdots}}} \quad (7)$$

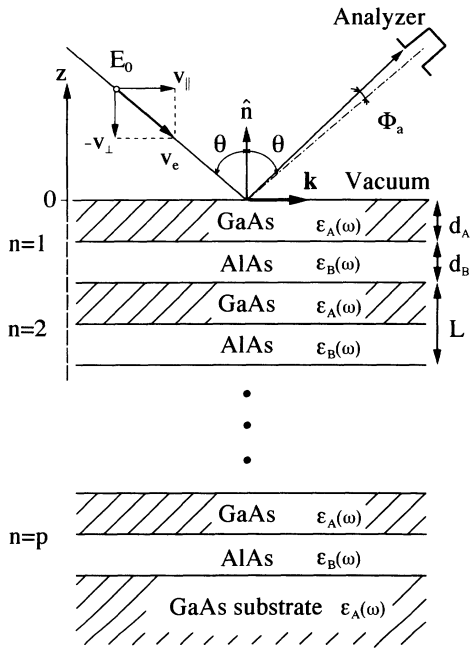

FIG. 1. Geometrical structure of the superlattice and the trajectory of an electron incident and scattered in a specular configuration. The GaAs and AlAs layers are deposited alternately on a GaAs substrate with thicknesses d_A and d_B. The topmost layer is GaAs. L is the thickness of one period ($L=d_A+d_B$) and p is the total number of the periods.

Here, a_n and b_n ($n=1\sim p$) are defined by

$$a_n=\frac{\varepsilon_n(\omega)}{\tanh(kd_n)} \quad \text{and} \quad b_n=\frac{\varepsilon_n(\omega)}{\sinh(kd_n)} , \tag{8}$$

respectively. $\varepsilon_n(\omega)$ and d_n are the dielectric function and the thickness of the nth layer, respectively. Since we assume that the superlattice is deposited on a semi-infinite GaAs substrate, i.e., $d_{p+1}=\infty$, we have $b_{p+1}=0$. Therefore, the continued fraction (7) has only a finite number of terms.

The dielectric functions for GaAs and AlAs in the frequency region (infrared) relevant to HREELS and Raman scattering are given by

$$\varepsilon_\nu(\omega)=\varepsilon_{\infty\nu}+\frac{(\varepsilon_{0\nu}-\varepsilon_{\infty\nu})\omega_{\mathrm{TO}\nu}^2}{\omega_{\mathrm{TO}\nu}^2-\omega^2-i\Gamma_\nu\omega} , \tag{9}$$

where $\nu=A$ and B; $\omega_{\mathrm{TO}\nu}$ is the transverse-optical (TO) phonon frequency of material ν; Γ_ν is the damping constant; $\varepsilon_{0\nu}$ and $\varepsilon_{\infty\nu}$ are the static and optical dielectric constants, respectively.

In the numerical calculation of Eq. (9), $\varepsilon_{0\nu}$ and $\varepsilon_{\infty\nu}$ were taken from the literature.[10] The TO phonon frequencies and the damping constants were determined by Raman scattering for the individual samples as described in the next section.

III. EXPERIMENTS

A. Sample fabrication

The samples used in our experiments were grown on semi-insulating GaAs(001) substrates by MBE at the Electrotechnical Laboratory. Three types of superlattices, which we call samples A, B, and C, were fabricated with their structural constants listed in Table I. They have different values of d_A and d_B, but have common values of $L=408$ Å and $p=10$.

Prior to the growth of the superlattices, the growth rates for GaAs and AlAs were determined to be approximately 1 and 0.5 monolayer/s, respectively, by observing the period of the intensity oscillation of reflection high-energy electron diffraction (RHEED).[11] All the superlattices were grown by opening the shutters in front of the Ga and Al sources alternately without surface recovery time. The precision of the layer thickness determination was empirically around 5%. After the growth, the samples were cooled down below 0 °C, and then their surfaces were exposed to As_4 beam for 20 min to form an As capping layer.[12]

TABLE I. Structural parameters of the superlattices, which are determined by RHEED.

Sample	d_1 (Å)	d_2 (Å)	L (Å)	p
A	102	306	408	10
B	204	204	408	10
C	306	102	408	10

B. Raman-scattering measurements

Raman measurements were carried out for all three samples of the superlattices to determine the TO phonon frequencies and the damping constants. The Raman spectra were measured in the $z(x,y)\bar{z}$ configuration, where x, y, and z directions are taken along the [100], [010], and [001] axes of the crystal, respectively. The 5145-Å line of an argon-ion laser was used at a power level of 300 mW for samples A and B, and 500 mW for sample C. The scattered light was analyzed by a double-grating spectrometer (Jobin-Yvon U-1000) with a resolution of 2 cm^{-1}.

Since the Raman tensors for the T_d symmetry crystals of GaAs and AlAs are given by[13]

$$F(x)=\begin{bmatrix}0&0&0\\0&0&d\\0&d&0\end{bmatrix} ,$$

$$F(y)=\begin{bmatrix}0&0&d\\0&0&0\\d&0&0\end{bmatrix} , \tag{10}$$

$$F(z)=\begin{bmatrix}0&d&0\\d&0&0\\0&0&0\end{bmatrix} ,$$

only the longitudinal-optical (LO) phonons are allowed in the configuration of our measurements. The TO phonon frequencies were obtained from the Lyddane-Sachs-Teller relation, using $\varepsilon_{0\nu}$, $\varepsilon_{\infty\nu}$, and the LO phonon frequency $\omega_{\mathrm{LO}\nu}$.

To determine the damping constants from the Raman spectra, the spectral broadening due to instrumental origins must be removed. The observed spectral shape $I(\omega)$ is the convolution of the true spectral shape $T(\omega)$ of the LO phonon and the spectrometer transmission function $F(\omega)$

$$I(\omega)=\int_{-\infty}^{+\infty} F(\omega-\omega')T(\omega')d\omega' . \tag{11}$$

$F(\omega)$ was obtained by measuring the spectrum of the 5145-Å laser line using the same spectrometer resolution of 2 cm^{-1}. Then, by deconvoluting $T(\omega)$ from $I(\omega)$, we obtained the damping constants.

C. HREELS

The HREELS measurements were carried out in an aluminum ultrahigh-vacuum chamber with a base pressure better than 3×10^{-8} Pa. The monochromator and the analyzer were home-made double-pass 127° cylindrical type designed after Oshima, Franchy, and Ibach.[14] After introducing the sample from air into the chamber, it was baked at 120 °C for 24 h and was cooled down to room temperature. Then, the pressure in the chamber reached the base pressure, and we started a procedure for removing the As capping layer.[15] First, the sample was annealed at 200 °C for 24 h. At this temperature, water, hydrocarbon, and oxygen molecules adsorbed on the As overlayer were desorbed.[16] Then, the sample was annealed at 250 °C for 6 h. The As overlayer starts to

desorb at this temperature. Finally, the As capping layer was removed thoroughly by heating the samples several times up to 450 °C for 1 min. Then, a mirrorlike surface was obtained.

The surface structure of each sample at this stage was observed by low-energy electron diffraction (LEED). Figure 2 shows a typical photograph of the LEED pattern. We see a (1×4) structure with streaks in the half-order positions along the [110] direction. This LEED pattern is similar to Fig. 7(b) of Ref. 15.

All HREEL spectra were measured in a specular configuration with the incident angle at 72° measured from the surface normal. The electron impact energy E_0 was varied from 4 to 35 eV. The typical electron counting rate of the elastic peak was $\sim 1\times 10^4$ cps and the energy resolution was ~ 50 cm^{-1}. The angular spread of the elastic peak was about 1° at full width at half maximum. This narrow angular spread indicates the presence of a well-ordered sample surface.

IV. RESULTS

A. Raman scattering

Figure 3 shows the Raman spectra of samples *A*, *B*, and *C*. We see Raman peaks for all the samples at 292 and 403 cm^{-1} that coincide with the LO phonon frequencies of GaAs and AlAs crystals, respectively. No TO phonon was observed at all. This means that the GaAs and AlAs layers were grown epitaxially with T_d symmetry. Table II shows the TO phonon frequencies and the damping constants determined by the procedure described in Sec. III along with other parameters required for the theoretical calculation of HREEL spectra.

B. HREELS

Figure 4 shows the HREEL spectra of sample *A* for electron impact energies of 4, 20, and 35 eV. All the intensities are normalized at their elastic-peak value. We see two dominant peaks at 290 and 385 cm^{-1} for all the impact energies. The ratio of the intensity at 290 cm^{-1} to that at 385 cm^{-1} decreases drastically as the electron impact energy increases. We can also see two loss peaks

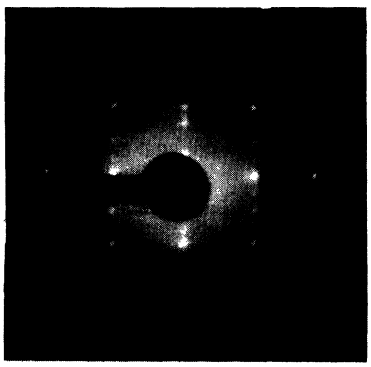

FIG. 2. LEED pattern of the superlattice after removing the As capping layer. A well-ordered GaAs(001) surface is obtained.

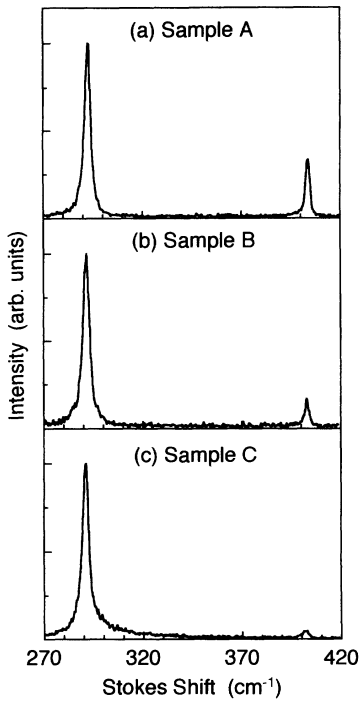

FIG. 3. Raman spectra of samples *A*, *B*, and *C* measured in the $z(x,y)\bar{z}$ configuration. The *x*, *y*, and *z* directions are taken along the [100], [010], and [001] axes of the samples, respectively.

at 580 and 760 cm^{-1} that correspond to the second-order harmonics of the peaks at 290 and 385 cm^{-1}, respectively, and a peak at 670 cm^{-1} that corresponds to the combination scattering of 290 and 385 cm^{-1}. Similar spectra were obtained for the other two samples, as shown in Figs. 7 and 8 below along with the theoretical results described in the next section.

V. DISCUSSION

In this section we will compare the experimental results of HREELS with the dielectric theory described in Sec. II, and discuss the physical origins of the loss peaks. In the comparison we must take into account the spectral broadening due to the finite-energy resolution of the HREELS spectrometer. The experimental results are compared with the theoretical results calculated by

$$P(\omega)=\int_{-\infty}^{+\infty} F(\omega-\omega')P_i(\omega')d\omega' , \tag{12}$$

where $F(\omega)$ is the instrumental broadening function, which is taken from the measured elastic-peak profile.

Figure 5 shows the comparison of the experimental result for sample *A* for the electron impact energy of 20 eV with the theoretical results for varied thicknesses of the GaAs layers d_A from 85 to 108 Å. The thickness step of 5.66 Å corresponds to two monolayers of GaAs. The intensity ratio between the loss peaks at 290 and 385 cm^{-1} is very sensitive to the thickness of the GaAs layer. We see that the experimental result agrees with the theoretical curve for the GaAs thickness of $d_A=96$ Å. Since the thickness determined by RHEED intensity oscillation

TABLE II. Dielectric parameters of GaAs and AlAs for samples *A*, *B*, and *C*.

	GaAs				AlAs			
Sample	ε_0	ε_∞	ω_{TO} (cm^{-1})	Γ (cm^{-1})	ε_0	ε_∞	ω_{TO} (cm^{-1})	Γ (cm^{-1})
A	12.91	10.9	267.3	3.5	10.06	8.16	362.9	2.1
B	12.91	10.9	267.7	3.6	10.06	8.16	362.8	2.0
C	12.91	10.9	267.6	3.6	10.06	8.16	362.9	3.1

was 102 Å, this result means that the fabricated GaAs layer is thinner by two monolayers than the designed value. The same fitting procedure was carried out for sample *B*, whose GaAs layer thickness is twice that of sample *A*. We obtained the best fitting value that is thinner by four monolayers than the designed value. These results show that the actual thickness of the GaAs layer was lower by 5% than that determined by the RHEED intensity oscillation. This result is consistent with the empirical precision of the layer thickness determination during the sample growth.

For sample *C*, we could not determine the thickness of the GaAs layers by the same method, because the intensity of the loss peak at 385 cm^{-1} was so weak that the fitting procedure could not be used. For this sample, we assumed that the thickness of the GaAs layer is thinner than the designed value by the same factor as determined above (-5%).

The theoretical spectra are not sensitive to the thickness of the AlAs layers. Thus, for AlAs we used the thickness determined by RHEED for the theoretical calculations.

In addition to the above estimation of the layer thicknesses, we must consider the effect of interface mixing. The theory employed in the present work assumes only sharp and abrupt interfaces. However, the actual superlattice may have diffuse interfaces where Ga and Al are intermixed. One may expect some intermixing to occur, since we did not allow surface recovery time in the growth process. This interface mixing can be simulated by inserting a ternary alloy $Al_xGa_{1-x}As$ as an intermixing layer between the GaAs and AlAs layers. The calculated spectra in this model are not sensitive to the thickness of the intermixing layer, if the interdiffusion distance is a few monolayers. This result shows that the abruptness of the interfaces cannot be tested by HREELS for the superlattices with layer thickness used in the present work. For superlattices with the layer thickness on the order of a few monolayers, the effect of the interface mixing will be detectable by HREELS.[17] Furthermore, even when a thick intermixing layer is considered, the calculated spectra do not agree with the experimental results. Thus, we neglected the effect of the interface mixing in the calculations of the HREEL spectra.

Figures 6, 7, and 8 show the HREEL spectra with the theoretical curves calculated by using the parameters determined above for samples *A*, *B*, and *C*, respectively. We see that excellent agreements are achieved for all samples with different layer thicknesses, and for all electron impact energies. Thus, we see that the dielectric

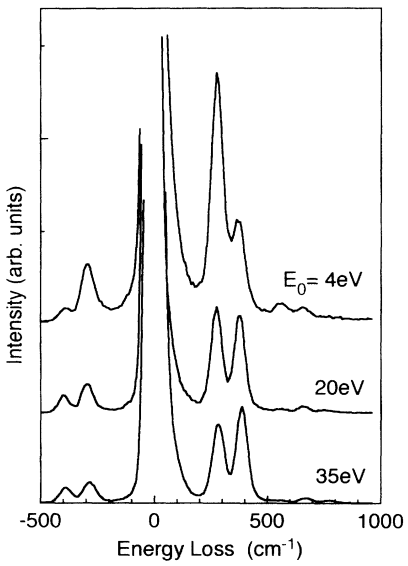

FIG. 4. HREEL spectra of sample *A*. E_0 is the electron impact energy.

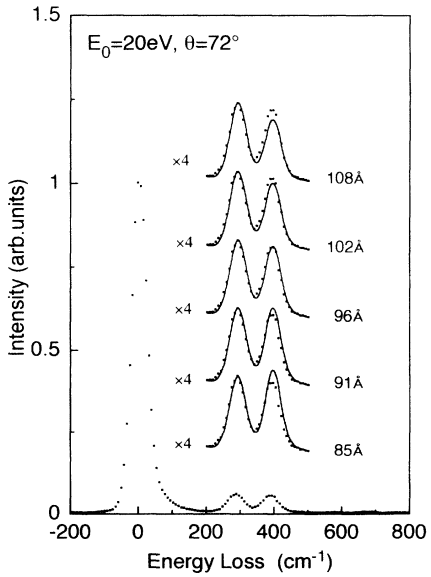

FIG. 5. Comparison between the experimental and theoretical results for sample *A*. The electron impact energy is fixed at 20 eV, and the thickness of the GaAs layers are varied from 85 to 108 Å with a step of 5.66 Å (two monolayers of GaAs) in the calculations. The theoretical result for 96 Å agrees with the experiment.

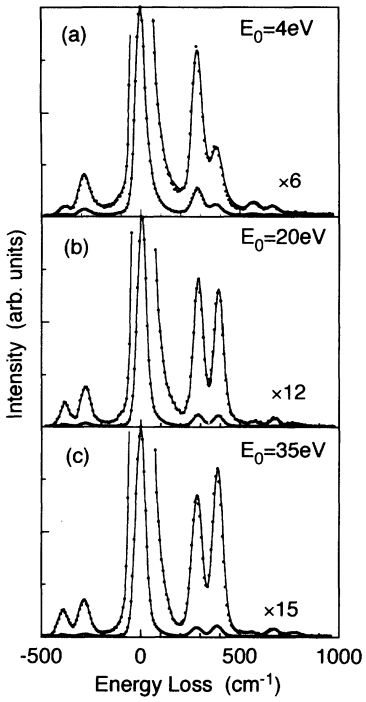

FIG. 6. Comparison of HREEL spectra of sample A (points) with the theoretical results (full curve) for incident energies from 4 to 35 eV.

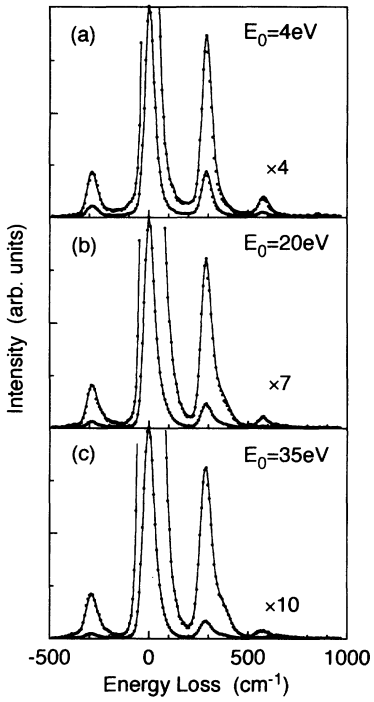

FIG. 8. Comparison of HREEL spectra of sample C (points) with the theoretical results (full curve) for incident energies from 4 to 35 eV.

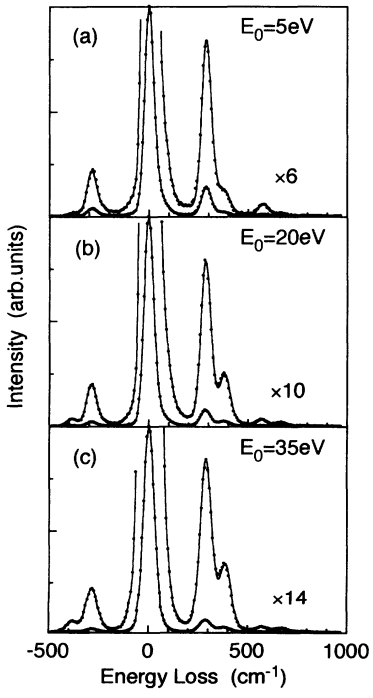

FIG. 7. Comparison of HREEL spectra of sample B (points) with the theoretical results (full curve) for incident energies from 4 to 35 eV.

theory can describe the HREEL spectra of the superlattices extremely well.

Now, let us discuss the physical origins of the individual loss peaks. Figure 9 shows the dispersion curves of the surface phonon polaritons for sample A. The finite number of the periods was taken into account in calculating these curves.[18] The dispersion curves represented by solid lines are attributed to the bulk modes that are distributed inside the superlattice. Two broken lines are the dispersion curves of the interface modes that are localized at the interface between the bottom AlAs layer and the GaAs substrate. These two modes do not appear in the HREEL spectra, because the electric fields of these modes are very weak in the vacuum above the sample surface.

The three modes plotted by single-dotted broken lines have strong electric fields in the vacuum above the sample surface, and interact strongly with the incident electrons. The mode around 290 cm^{-1} is the surface mode that is localized at the top surface of the superlattice. (Recall that the top layer is GaAs.) This mode has the asymptotic frequency determined by $\varepsilon_A(\omega)=-1$. This is the general condition for the usual surface modes. The two modes around 280 and 390 cm^{-1} are localized at the interface between the topmost GaAs layer and the second AlAs layer, and have the asymptotic frequencies determined by $\varepsilon_A(\omega)=-\varepsilon_B(\omega)$ for $k\rightarrow\infty$. These interface modes are the intrinsic modes of the superlattice and not

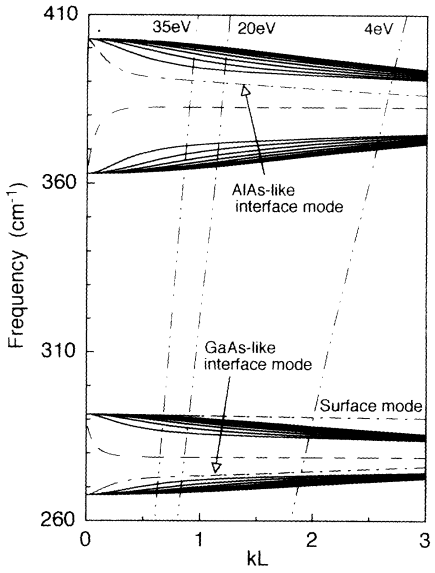

FIG. 9. The dispersion curves of surface and interface phonon polaritons in the GaAs(96 Å)-AlAs(102 Å) superlattice. The three modes indicated by dotted-dashed lines have strong electric fields in the vacuum above the sample surface. The double-dotted–dashed lines show the relation $kL=\omega/v_{\parallel}L$ for the electron impact energies 4, 20, and 35 eV.

of a single interface structure, because these modes are formed by a superposition of the fields of the interface modes excited at individual interfaces. Since these two modes lie in the frequency regions in which GaAs and AlAs become surface-wave active, respectively, we will call the former the "GaAs-like interface mode" and the latter the "AlAs-like interface mode."

From the dispersion relations of Fig. 9, we can identify the loss peaks that we observed. The peak at 385 cm^{-1} is attributed to the AlAs-like interface mode and the peak at 290 cm^{-1} is attributed to both the surface mode and the GaAs-like interface mode. These two modes could not be resolved because of the low-energy resolution of the HREELS spectrometer.

The electron-impact-energy dependence of the energy positions of these two peaks can also be understood from the dispersion relations. In Fig. 9, we drew three lines of the maximum of the kinematic prefactor in Eq. (4) for the electron impact energies of 4, 20, and 35 eV. On these lines, the surface parallel component of the electron velocity coincides with the phase velocity of the surface polaritons. Therefore, the incident electrons interact strongly with the surface polaritons that have ω and k around the cross points of these lines with the dispersion curves. As seen in Fig. 9, the frequencies of the cross points shift only by a few cm^{-1} for the electron impact energies from 4 to 35 eV. Thus, the loss-peak positions do not show any electron-impact-energy dependence when the energy resolution is not sufficiently high.

Finally, we wish to remark on the effectiveness of the combined HREELS-Raman study on superlattices. HREELS has high sensitivity to the surface and interface excitations, and the properties of the layers that compose the superlattice structure. If the layer thickness is less than about 200 Å, one can determine the thickness of the topmost layer with a precision on the order of two monolayers as demonstrated in Fig. 5. On the other hand, Raman scattering has high-energy resolution and polarization selection rules, and sees the bulk excitations inside the superlattice. Thus, one can confirm the crystallinity of the samples, and determine precisely the dielectric parameters that are needed for the theoretical calculations. By complementing the features of the two methods, we have obtained excellent agreement between the theory and the experiment.

VI. CONCLUSION

We have measured the HREEL spectra of GaAs-AlAs superlattices and compared them with the calculated results from the dielectric theory. The TO phonon frequencies and the damping constants for the GaAs and AlAs layers were determined for individual samples *in situ* from the Raman spectra. These input parameters were used in calculating the theoretical dispersion curves and the HREEL spectra. Excellent agreement was obtained between the theory and the experiment for all the samples with different layer thicknesses, and for all the electron impact energies (from 4 to 35 eV). We conclude that the dielectric theory gives an excellent description of the normal modes and their electron-scattering properties of the GaAs-AlAs superlattices.

ACKNOWLEDGMENTS

We would like to thank Professor C. Oshima of Waseda University for his advice on the design of our electron-energy-loss spectroscopy (EELS) system. We wish to acknowledge important contributions by T. Wakamatsu of Ibaraki National College of Technology and S. Mori of Canon, Inc., in the construction of the EELS system in our laboratory. Also, we would like to acknowledge the excellent technical support provided by the Machine Shop of our Institute. We thank Dr. K. Sakamoto for technical assistance in the Raman measurements. This work was supported in part by a Grant-in-Aid for Scientific Research from the Ministry of Education, Science, and Culture.

*Present address: Advanced Materials and Technology Research Laboratories, Nippon Steel Corp., 1618 Ida, Nakahara-ku, Kawasaki 211, Japan.

[1]S. Andersson and B. N. J. Persson, Phys. Rev. Lett. **45**, 1421 (1980).

[2]M. Liehr, P. A. Thiry, J. J. Pireaux, and R. Caudano, J. Vac. Sci. Technol. A **2**, 1079 (1984).

[3]Ph. Lambin, J. P. Vigneron, and A. A. Lucas, Phys. Rev. B **32**, 8203 (1985).

[4]P. A. Thiry, M. Liehr, J. J. Pireaux, R. Caudano, Ph. Lambin,

J. P. Vigneron, A. A. Lucas, and T. J. Kuech, J. Vac. Sci. Technol. B **4**, 1023 (1986).

[5]P. A. Thiry, J. L. Longueville, J. J. Pireaux, R. Caudano, H. Munekata, and M. Liehr, J. Vac. Sci. Technol. A **5**, 603 (1987).

[6]Z. J. Gray-Grychowski, R. G. Egdell, B. A. Joyce, R. A. Stradling, and K. Wooddbridge, Surf. Sci. **186**, 482 (1987).

[7]A. A. Lucas and M. Sunjic, in *Progress in Surface Science,* edited by S. G. Davidson (Pergamon, London, 1972), Vol. 2, p. 75.

[8]H. Ibach and D. L. Mills, *Electron Energy Loss Spectroscopy and Surface Vibrations* (Academic, New York, 1982).

[9]Ph. Lambin, A. A. Lucas, and J. P. Vigneron, Surf. Sci. **182**, 567 (1987).

[10]M. Cardona and G. Harbeke, in *III-V Compounds,* edited by O. Madelung, Landolt-Börnstein, New Series, Group III, Vol. 17, pt. a (Springer, Berlin, 1982).

[11]T. Sakamoto, H. Funabashi, K. Ohta, T. Nakagawa, N. Kawai, and T. Kojima, Jpn. J. Appl. Phys. **23**, L657 (1984).

[12]N. J. Kawai, T. Nakagawa, T. Kojima, K. Ohta, and M. Kawashima, Electron. Lett. **20**, 47 (1984).

[13]R. Loudon, Adv. Phys. **13**, 423 (1964).

[14]C. Oshima, R. Franchy, and H. Ibach, Rev. Sci. Instrum. **54**, 1024 (1983).

[15]R. W. Bernstein, A. Borg, H. Husby, B. O. Fimland, and J. K. Grespstad, Appl. Surf. Sci. **56-57**, 74 (1992).

[16]B. J. Schafer, A. Forster, M. Londschien, A. Tulke, K. Werner, M. Kamp, H. Heinecke, M. Weyers, and H. Lüth, Surf. Sci. **204**, 482 (1988).

[17]P. Senet, Ph. Lambin, and A. A. Lucas, Surf. Sci. **269/270**, 141 (1992).

[18]B. L. Johnson, J. T. Weiler, and R. E. Camley, Phys. Rev. B **32**, 6544 (1985).

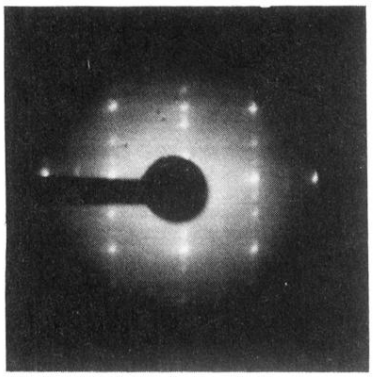

FIG. 2. LEED pattern of the superlattice after removing the As capping layer. A well-ordered GaAs(001) surface is obtained.